Available online at www.sciencedirect.com
SCIENCE DIRECT®
Journal of Hydrology 317 (2006) 239–260
Journal of Hydrology
www.elsevier.com/locate/jhydrol

General well function for pumping from a confined, leaky, or unconfined aquifer

Tomas Perina[a,*], Tien-Chang Lee[b,1]

[a] CH2M HILL, 3550 Vine Street Suite 320, Riverside, CA 92507, USA
[b] Department of Earth Sciences, University of California, Riverside, CA 92521, USA

Received 26 November 2003; revised 10 May 2005; accepted 25 May 2005

Abstract

A general well function for groundwater flow toward an extraction well with non-uniform radial flux along the screen and finite-thickness skin, partially penetrating an unconfined, leaky-boundary flux, or confined aquifer is derived via the Laplace and generalized finite Fourier transforms. The mixed boundary condition at the well face is solved as the discretized Fredholm integral equation. The general well function reduces to a uniform radial flux solution as a special case. In the Laplace domain, the relation between the drawdown in the extraction well and flowrate is linear and the formulations for specified flowrate or specified drawdown pumping are interchangeable. The deviation in drawdown of the uniform from non-uniform radial flux solutions depends on the relative positions of the extraction and observation well screens, aquifer properties, and time of observation. In an unconfined aquifer the maximum deviation occurs during the period of delayed drawdown when the effect of vertical flow is most apparent. The skin and wellbore storage in an observation well are included as model parameters. A separate solution is developed for a fully penetrating well with the radial flux being a continuous function of depth.

Keywords: Unconfined aquifer; Leaky aquifer; Constant flowrate pumping; Constant drawdown pumping; Well function; Mixed type boundary condition

1. Introduction

New analytical solution for groundwater flow toward a partially penetrating well of finite diameter installed in an unconfined, leaky, or confined aquifer of finite thickness under a variety of test conditions is here presented. The solution allows for non-uniform radial flux distribution along the well screen. It is applicable to specified flowrate or specified drawdown pumping from a partially penetrating well surrounded by a skin zone.

Flow toward a partially penetrating well has usually been treated with the assumption of a uniform radial flux (UF) along the well screen for the development of analytical solutions (e.g.: Hantush, 1961; Neuman, 1974; Lee, 1999). It is more appropriate to assume that the pressure change induced by extraction occurs instantaneously within

* Corresponding author. Tel.: +1 951 276 3003x24; fax: +1 714 424 2204.
E-mail addresses: tperina@ch2m.com (T. Perina), tien.lee@ucr.edu (T.-C. Lee).
[1] Tel.: +1 951 827 4506; fax: +1 951 827 4324.

0022-1694/$ - see front matter © 2005 Elsevier B.V. All rights reserved.
doi:10.1016/j.jhydrol.2005.05.020

Nomenclature

a	factor resulting from the upper boundary condition, $a = S_y pb/K_z$
b	saturated thickness, [m]
b_c	thickness of confining layer, [m]
c_v	vertical leakance of confining layer, [s^{-1}]
H	drawdown within the extraction well, [m]
H_c	constant drawdown applied at the extraction well, [m]
H_d	initial displacement applied within the tested well during slug test, [m]
h^a	drawdown within the aquifer, [m]
h_{os}	average drawdown along the aquifer-observation well skin interface, [m]
h_{ow}	drawdown in observation well casing, [m]
h^s	drawdown within the well skin, [m]
K_n	modified Bessel function of the first kind and n-th order, [−]
I_n	modified Bessel function of the second kind and n-th order, [−]
K_c	vertical hydraulic conductivity of confining layer, [ms^{-1}]
K_{os}	hydraulic conductivity of observation well skin, [ms^{-1}]
K_r	horizontal hydraulic conductivity, [ms^{-1}]
K_z	vertical hydraulic conductivity, [ms^{-1}]
N	number of well screen segments, [−]
N_{sin}	nearest integer of $2/\Delta\eta$
p	Laplace transform variable ($t \rightarrow p$), [s^{-1}]
Q	extraction rate, [$m^3\ s^{-1}$]
Q_c	constant flowrate from the extraction well, [$m^3\ s^{-1}$]
q	specific radial flux across the pumping well screen per unit screen length, [$m^2\ s^{-1}$]
q_j	specific radial flux across the j-th screen segment, [$m^2\ s^{-1}$]
r	radial distance, [m]
r_c	radius of extraction well casing, [m]
r_{oc}	radius of observation well casing, [m]
r_{os}	radius of observation well skin, [m]
r_{ow}	radius of observation well screen, [m]
r_s	radius of skin, [m]
r_w	radius of extraction well screen, [m]
S_s	specific storage, [m^{-1}]
S_y	specific yield, [−]
t	time, [s]
z	depth below the top of the aquifer, [m]
z_b	z to the bottom of the extraction well screen, [m]
z_{ob}	z to the bottom of observation well screen, [m]
z_{ot}	z to the top of observation well screen, [m]
z_t	z to the top of the extraction well screen, [m]
α	factor resulting from the wellbore storage condition, $\alpha = \pi r_c^2 p$
$\Delta\eta_j$	dimensionless length of the j-th screen segment, [−]
η	dimensionless depth $\eta = (b-z)/b$, [−]
λ_n	roots of (24)
ξ_n	quantity resulting from the modified Bessel Eq. (30), [m^{-1}]

The overbar stands for the Laplace transform and subscript n for the GFFC transform. Superscripts a and s stand for properties of the aquifer and skin, respectively.

the well, and to use a mixed type boundary condition at r_w; i.e. with specified drawdown along the screen and zero flux elsewhere (Hyder et al., 1994; Cassiani and Kabala, 1998; Hemker, 1999; Chang and Chen, 2003). Several authors recently presented analytical solutions for a mixed-boundary problem of constant drawdown pumping from a well partially penetrating a confined aquifer. Their solutions account for non-uniform radial flux (NUF) along the extraction well screen. Cassiani and Kabala (1998) presented a solution for a flowing partially penetrating well in a confined aquifer of semi-infinite vertical extent. Chang and Chen (2003) derived a solution for constant drawdown pumping test conducted on a well partially penetrating a confined aquifer of finite thickness. Hemker (1999) presented a hybrid analytical-numerical solution for flow in a layered aquifer toward a well operated at a specified discharge that accounts for non-uniform radial flow distribution along the screen. Lee and Damiata (1995) solved an equivalent mixed-boundary condition problem in downhole resistivity logging to account for constant

voltage and varying radial current transmission along an electrode of finite length.

The boundary condition at the well face is of mixed-type for either specified drawdown or specified flowrate pumping test. It will be shown in this paper that the relation between the drawdown in the extraction well and the pumping rate is linear in the Laplace domain and solutions for drawdown during specified flowrate pumping and specified drawdown pumping can be derived from a single formulation. Constant flowrate pumping, constant drawdown pumping, and slug test are presented as special cases. The solution for constant drawdown pumping from a partially penetrating well can be derived for both UF and NUF models.

The NUF solution for a partially penetrating well is derived using a discretization approach similar to the one used by Chang and Chen (2003) and Lee and Damiata (1995); the solution can, therefore, be classified as 'semi-analytical'. We also derive a NUF solution for a well fully penetrating an unconfined or leaky aquifer without the discretization and with the radial flux across the well screen being a continuous function of depth; this solution serves also as an accuracy check for the discretization approach. Our solution constitutes a general well function for pumping from a uniform confined aquifer of Theis (1935), unconfined aquifer of Neuman (1972), and leaky-boundary flux aquifer of Lee (1999, p. 134).

2. Formulation of solutions

Consider a Neuman's (1972, 1973) type of unconfined aquifer of thickness b. Its properties (K_r^a, K_z^a, S_s^a, S_y^a and b) are uniform within the zone influenced by the pumping. Aquifer drainage at the water table is presumably instantaneous. The drawdown is sufficiently small, so that the position of the water table can be assumed to be unchanged during the test for mathematical convenience. Confined and leaky aquifers will be considered later as special cases. The initial condition is taken as zero drawdown everywhere in the aquifer prior to the test.

The extraction well has a finite diameter and partially penetrates the aquifer (Fig. 1). The test is conducted under the condition of either specified flowrate or specified drawdown instantaneously applied at the extraction well at time zero. The term 'specified' implies that the quantity be known (or measured); in general, it does not have to be constant in time.

Wellbore storage effect and low permeability skin at the extraction well (Mishra and Guyonnet, 1992;

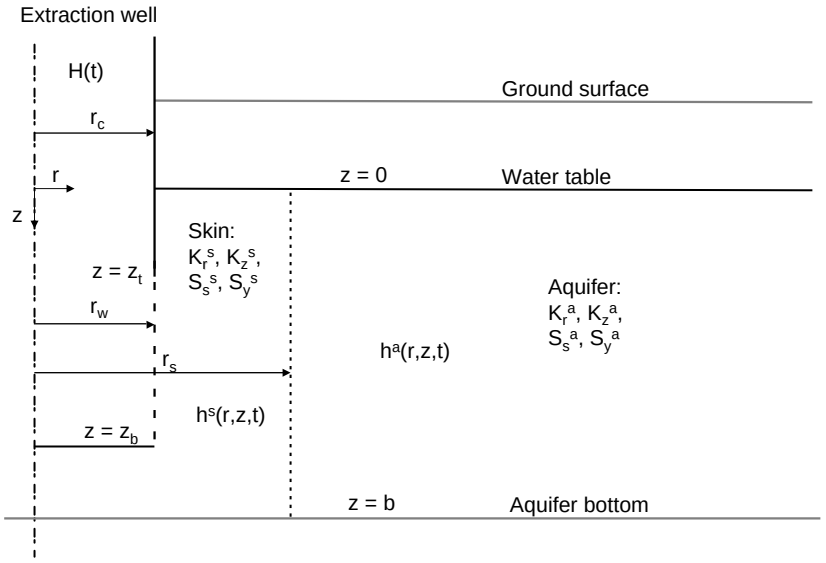

Fig. 1. Test well geometry in an unconfined aquifer of thickness b.

Moench, 1997, 1998; Lee, 1999) and observation well (Black and Kipp, 1977; Tongpenyai and Raghavan, 1981; Shapiro, 1989) will be considered here. Effects of nonlinear frictional well losses (Kawecki, 1995) and water level changes in wells due to atmospheric pressure fluctuations and earth tides (Rasmussen and Crawford, 1997) can be removed from the test data by applying additional corrections.

A finite thickness skin with properties K_r^s, K_z^s, S_y^s, and S_s^s extending from r_w to r_s ($r_s > r_w$) is considered. Superscripts a and s used to designate the properties of the aquifer and skin, respectively, are omitted in relations that hold for both regions.

The governing partial differential equation for density-independent groundwater flow is

$$K_r\left[\frac{\partial^2 h}{\partial r^2}+\frac{1}{r}\frac{\partial h}{\partial r}\right]+K_z\frac{\partial^2 h}{\partial z^2}=S_s\frac{\partial h}{\partial t}, \tag{1}$$

where h is the drawdown as a function of time (t) and position and K_r and K_z are the hydraulic conductivities in the radial and vertical directions, respectively, and S_s is the specific storage (see the list of Nomenclature).

The boundary conditions vary depending on the type of aquifer, screen placement of the extraction well, and type of test (specified extraction rate, specified drawdown, or slug test). The general well face boundary condition is

$$f(z)\left[Q-\pi r_c^2\frac{\partial H}{\partial t}\right]=-2\pi r_w K_r\int_{z_t}^{z_b}\frac{\partial h}{\partial r}\mathrm{d}z \quad \text{at } r=r_w, \tag{2}$$

where

$$f(z)=\begin{cases}1 & z_t\le z\le z_b\\ 0 & \text{otherwise}\end{cases}, \tag{3}$$

Q is the extraction rate, r_w is the well screen radius, r_c is the well casing radius (in general, the two radii may be different), H is the drawdown within the extraction well, and z_t and z_b are depths to the top and bottom of the well screen, respectively (the z coordinate is downward positive).

The groundwater flow region is divided into two zones in the radial direction: $r_s \le r < \infty$ for flow in the aquifer and $r_w \le r < r_s$ for flow within the skin. To impose continuity of drawdown and flux at the joint boundary at r_s, the drawdown in the aquifer h^a and within the skin h^s are related by

$$h^s = h^a \quad \text{at } r=r_s \tag{4}$$

and

$$K_r^s\frac{\partial}{\partial r}h^s = K_r^a\frac{\partial}{\partial r}h^a \quad \text{at } r=r_s. \tag{5}$$

It is convenient to re-write the well face boundary condition (2) as

$$q=-2\pi r_w K_r^s\frac{\partial h^s}{\partial r} \quad \text{at } r=r_w \tag{6}$$

where q is the yet unknown radial flux per unit screen length and satisfy the condition for wellbore storage by

$$Q-\pi r_c^2\frac{\partial H}{\partial t}=\int_{z_t}^{z_b} q\mathrm{d}z. \tag{7}$$

The pumping test problem is defined by the governing Eq. (1) subject to the initial condition

$$h=0 \quad \text{at } t=0, \tag{8}$$

boundary conditions

$$K_z\frac{\partial h}{\partial z}=S_y\frac{\partial h}{\partial t} \quad \text{at } z=0, \tag{9}$$

$$\frac{\partial h}{\partial z}=0 \quad \text{at } z=b, \tag{10}$$

$$h^a\to 0 \quad \text{as } r\to\infty, \tag{11}$$

well-face condition (6), and wellbore storage condition (7). It is noted that because boundary condition (9) is of the Cauchy type, vertical flow will occur in the aquifer during pumping from either a partially or fully penetrating extraction well.

2.1. Solution

Take the Laplace transform in time of Eq. (1), initial condition (8), boundary conditions (6), (9)–(11), as well as condition (7). Then, introduce a dimensionless variable,

$$\eta=\frac{b-z}{b}, \tag{12}$$

for the convenience of an integral transform to be applied later. These equations become:

$$K_r\left[\frac{\partial^2\bar{h}}{\partial r^2}+\frac{1}{r}\frac{\partial\bar{h}}{\partial r}\right]+\frac{K_z}{b^2}\frac{\partial^2\bar{h}}{\partial\eta^2}=S_s p\bar{h}, \tag{13}$$

$$-\frac{K_z}{b}\frac{\partial\bar{h}}{\partial\eta}=S_y p\bar{h} \quad \text{at } \eta=1, \tag{14}$$

$$\frac{\partial\bar{h}}{\partial\eta}=0 \quad \text{at } \eta=0, \tag{15}$$

$$\overline{h^a}\to 0 \quad \text{as } r\to\infty, \tag{16}$$

$$\bar{q}=-2\pi r_w K_r^s\frac{\partial\overline{h^s}}{\partial r} \quad \text{at } r=r_w, \tag{17}$$

$$\overline{h^s}=\overline{h^a} \quad \text{at } r=r_s, \tag{18}$$

$$K_r^s\frac{\partial}{\partial r}\overline{h^s}=K_r^a\frac{\partial}{\partial r}\overline{h^a} \quad at \quad r=r_s, \tag{19}$$

and

$$\bar{Q}-\alpha\bar{H}=b\int_{\eta_1}^{\eta_2}\bar{q}\,d\eta, \tag{20}$$

where

$$\alpha=\pi r_c^2 p, \tag{21}$$

$$\eta_1=\frac{b-z_b}{b}, \qquad \text{and } \eta_2=\frac{b-z_t}{b}. \tag{22}$$

Eq. (13) is to be solved by means of the generalized finite Fourier cosine (GFFC) transform defined on the interval $0\le x\le 1$ (Churchill, 1972, p. 370). The nth term of GFFC is

$$g_n=F\{g(x)\}=\int_0^1 g(x)\cos(\lambda_n x)dx, \tag{23}$$

where λ_n are the roots of

$$\tan(y)=\frac{a}{y}, \tag{24}$$

and a is a positive constant, to be related later to aquifer properties. Using the relation (24), the eigenfunction $\cos(\lambda_r x)$ can be shown to have the orthogonality property

$$\int_0^1\cos(\lambda_n x)\cos(\lambda_m x)dx=\begin{cases}0, & n\neq m\\ \dfrac{a+\sin^2(\lambda_n)}{2a}, & n=m\end{cases}. \tag{25}$$

Accordingly, the inversion formula is

$$g(x)=F^-\{g_n\}=2a\sum_{n=0}^{\infty}g_n\frac{\cos(\lambda_n x)}{a+\sin^2(\lambda_n)}. \tag{26}$$

The GFFC transform of the second derivative $\int_0^1\frac{\partial^2 g(x)}{\partial x^2}\cos(\lambda_n x)dx$,

$$F\left\{\frac{\partial^2}{\partial x^2}g(x)\right\}=-\lambda_n^2 g_n-\frac{\partial}{\partial x}g(0)+\left[ag(1)+\frac{\partial}{\partial x}g(1)\right]\cos(\lambda_n), \tag{27}$$

obtained by repeated integration by parts, makes it suitable for the unconfined problem considered because the top and bottom boundary conditions can be conveniently implemented.

It is noted that the GFFC transform can be replaced by a corresponding technique of separation of variables with generalized cosine series expansion (Churchill, 1972; p. 307). The finite cosine and sine transforms, commonly used to solve flow problems involving partially penetrating wells (e.g., Hantush, 1961; Hyder et al., 1994), cannot be used in this case because of the Cauchy-type boundary condition at the water table.

The top boundary condition is now rewritten as

$$\frac{\partial\overline{h^a}}{\partial\eta}+a^a\overline{h^a}=0 \quad \text{and} \quad \frac{\partial\overline{h^s}}{\partial\eta}+a^s\overline{h^s}=0 \quad \text{at } \eta=1, \tag{28}$$

$$a^a=\frac{S_y^a pb}{K_z^a} \quad \text{and} \quad a^s=\frac{S_y^s pb}{K_z^s}. \tag{29}$$

Roots λ_n^a and λ_n^s correspond to a^a and a^s, respectively.

Applying the GFFC transform in η, imposing the top and bottom boundary conditions, using the orthogonality of $\cos(\lambda_n x)$, and rearranging terms

results in

$$\frac{\partial^2 \bar{h}_n}{\partial r^2} + \frac{1}{r}\frac{\partial \bar{h}_n}{\partial r} - \left[\frac{K_z}{b^2}\frac{\lambda_n^2}{K_r} + \frac{S_s p}{K_r}\right]\bar{h}_n = 0 \tag{30}$$

for the n-th term of an infinite series.

The Fourier-transformed well face boundary condition is

$$\int_0^1 \bar{q}\cos(\lambda_n^s \eta)\mathrm{d}\eta = -2\pi r_w K_r^s \frac{\partial \bar{h}_n^s}{\partial r} \quad \text{at } r = r_w. \tag{31}$$

The left-hand side of (31) will be resolved later for $\bar{q}$. The transformed joint boundary conditions are

$$\overline{h_n^s} = \overline{h_n^a} \quad \text{at } r = r_s, \tag{32}$$

and

$$K_r^s \frac{\partial}{\partial r}\overline{h_n^s} = K_r^a \frac{\partial}{\partial r}\overline{h_n^a} \quad \text{at } r = r_s. \tag{33}$$

Solving Eq. (30) subject to transformed condition (16) yields

$$\overline{h_n^a} = C_n K_0(\xi_n^a r) \tag{34}$$

and

$$\overline{h_n^s} = B_n K_0(\xi_n^s r) + A_n I_0(\xi_n^s r) \tag{35}$$

where K_0 and I_0 are the modified Bessel functions of the first and second kinds and zeroth order,

$$\xi_n^a = \sqrt{\frac{K_z^a}{b^2}\frac{\lambda_n^{a2}}{K_r^a} + \frac{S_s^a p}{K_r^a}}, \tag{36}$$

and

$$\xi_n^s = \sqrt{\frac{K_z^s}{b^2}\frac{\lambda_n^{s2}}{K_r^s} + \frac{S_s^s p}{K_r^s}}. \tag{37}$$

Coefficients A_n and C_n are evaluated from conditions (32) and (33)

$$C_n = B_n \frac{K_0(\xi_n^s r_s)}{K_0(\xi_n^a r_s)} + A_n \frac{I_0(\xi_n^s r_s)}{K_0(\xi_n^a r_s)}, \tag{38}$$

$$A_n = B_n G_n, \tag{39}$$

where

$$G_n = \left[\frac{K_r^s \xi_n^s}{K_r^a \xi_n^a} K_1(\xi_n^s r_s) - \frac{K_0(\xi_n^s r_s) K_1(\xi_n^a r_s)}{K_0(\xi_n^a r_s)}\right] \times \left[\frac{K_r^s \xi_n^s}{K_r^a \xi_n^a} I_1(\xi_n^s r_s) + \frac{I_0(\xi_n^s r_s) K_1(\xi_n^a r_s)}{K_0(\xi_n^a r_s)}\right]^{-1}, \tag{40}$$

and K_1 and I_1 are the modified Bessel functions of the first and second kinds and first order.

It is now convenient to express the GFFC transformed solution as

$$\overline{h_n^a} = B_n \left[\frac{K_0(\xi_n^s r_s)}{K_0(\xi_n^a r_s)} + G_n \frac{I_0(\xi_n^s r_s)}{K_0(\xi_n^a r_s)}\right] K_0(\xi_n^a r) \tag{41}$$

and

$$\overline{h_n^s} = B_n [K_0(\xi_n^s r) + G_n I_0(\xi_n^s r)]. \tag{42}$$

Coefficient B_n is evaluated from condition (31)

$$B_n = \frac{\int_0^1 \bar{q}\cos(\lambda_n^s \eta)\mathrm{d}\eta}{2\pi r_w K_r^s \xi_n^s [K_1(\xi_n^s r_w) - G_n I_1(\xi_n^s r_w)]} \tag{43}$$

Eq. (43) containing the unknown flux $\bar{q}$ under the integral is the Fredholm integral equation of the first kind (Press et al., 1992, p. 779). It will be solved in a discrete form. The well screen interval is discretized into N segments of length $\Delta\eta_j$ which is sufficiently small that the radial flux $\bar{q}$ can be assumed to be constant within each segment. The segments do not need to be of equal length. As discussed later, the segmental length determines the number of the Fourier summation terms. The fluxes will be determined by imposing the condition of uniform drawdown along the well screen. Let $\bar{q}_j$ represent the unit flux per screen length from the aquifer into the well segment j; then the inegral can be replaced by the summation

$$B_n = \sum_{j=1}^{N} \bar{q}_j D_{j,n} \tag{44}$$

where

$$D_{j,n} = \frac{[\sin(\lambda_n^s \eta_{j+}) - \sin(\lambda_n^s \eta_{j-})]}{2\pi r_w K_r^s \lambda_n^s \xi_n^s [K_1(\xi_n^s r_w) - G_n I_1(\xi_n^s r_w)]}, \tag{45}$$

$$\eta_{j-} = \eta_j - \frac{\Delta\eta_j}{2}, \quad \eta_{j+} = \eta_j + \frac{\Delta\eta_j}{2}, \tag{46}$$

and

$$\Delta\eta_j = \eta_{j+} - \eta_{j-}. \tag{47}$$

Taking the inverse GFFC transform of (41) and (42) yields

$$\overline{h^{\mathrm{a}}} = 2a^{\mathrm{a}} \sum_{n=0}^{\infty} B_n \left[\frac{K_0(\xi_n^{\mathrm{s}} r_s)}{K_0(\xi_n^{\mathrm{a}} r_s)} + G_n \frac{I_0(\xi_n^{\mathrm{s}} r_s)}{K_0(\xi_n^{\mathrm{a}} r_s)} \right] K_0(\xi_n^{\mathrm{a}} r) \frac{\cos(\lambda_n^{\mathrm{a}} \eta)}{a^{\mathrm{a}} + \sin^2(\lambda_n^{\mathrm{a}})}, \tag{48}$$

and

$$\overline{h^{\mathrm{s}}} = 2a^{\mathrm{s}} \sum_{n=0}^{\infty} B_n [K_0(\xi_n^{\mathrm{s}} r) + G_n I_0(\xi_n^{\mathrm{s}} r)] \times \frac{\cos(\lambda_n^{\mathrm{s}} \eta)}{a^{\mathrm{s}} + \sin^2(\lambda_n^{\mathrm{s}})}. \tag{49}$$

Eqs. (48) and (49) still contain the unknown fluxes. The solution for radial flux is subject to the condition that the average drawdown at $r = r_{\mathrm{w}}$ for every segment is equal to $\bar{H}$. The drawdown $\bar{H}$ is calculated as an average along each screen segment i

$$\bar{H} = \frac{1}{\eta_{i+} - \eta_{i-}} \int_{\eta_{i-}}^{\eta_{i+}} \overline{h^{\mathrm{s}}} \mathrm{d}\eta \quad \text{at } r = r_{\mathrm{w}} \tag{50}$$

to obtain

$$\bar{H} = \frac{2a^{\mathrm{s}}}{\Delta\eta_i} \sum_{n=0}^{\infty} B_n \left[\frac{K_0(\xi_n^{\mathrm{s}} r_{\mathrm{w}}) + G_n I_0(\xi_n^{\mathrm{s}} r_{\mathrm{w}})}{a^{\mathrm{s}} + \sin^2(\lambda_n^{\mathrm{s}})} \right] \times \frac{\sin(\lambda_n^{\mathrm{s}} \eta_{i+}) - \sin(\lambda_n^{\mathrm{s}} \eta_{i-})}{\lambda_{\mathrm{n}}^{\mathrm{s}}}. \tag{51}$$

The system of Eq. (51) relates the unknown fluxes $\bar{q}_j$ to the drawdown in the extraction well H for a drawdown-controlled well (specified drawdown pumping). In matrix form for all segments, it becomes

$$\bar{H} = \sum_{j=1}^{N} \overline{q_j} \Psi_{ij}, \tag{52}$$

or explicitely

$$\begin{bmatrix} \Psi_{1,2} & \Psi_{1,2} & \cdots & \cdots & \Psi_{1,N} \\ \Psi_{2,1} & \Psi_{2,2} & \cdots & \cdots & \Psi_{2,N} \\ \vdots & \vdots & \vdots & \vdots & \vdots \\ \vdots & \vdots & \vdots & \vdots & \vdots \\ \Psi_{N,1} & \Psi_{N,2} & \cdots & \cdots & \Psi_{N,N} \end{bmatrix} \begin{bmatrix} \overline{q_1} \\ \overline{q_2} \\ \vdots \\ \vdots \\ \overline{q_N} \end{bmatrix} = \begin{bmatrix} \bar{H} \\ \bar{H} \\ \vdots \\ \vdots \\ \bar{H} \end{bmatrix}, \tag{53}$$

where

$$\Psi_{ij} = \frac{a^{\mathrm{s}}}{\pi r_{\mathrm{w}} K_{\mathrm{r}}^{\mathrm{s}} \Delta\eta_i} \times \sum_{n=0}^{\infty} \frac{K_0(\xi_n^{\mathrm{s}} r_{\mathrm{w}}) + G_n I_0(\xi_n^{\mathrm{s}} r_{\mathrm{w}})}{\xi_n^{\mathrm{s}} [K_1(\xi_n^{\mathrm{s}} r_{\mathrm{w}}) - G_n I_1(\xi_n^{\mathrm{s}} r_{\mathrm{w}})]} \times \frac{\psi_{ij}}{a^s + \sin^2(\lambda_n^{\mathrm{s}})} \tag{54}$$

and

$$\psi_{ij} = \frac{[\sin(\lambda_n^{\mathrm{s}} \eta_{j+}) - \sin(\lambda_n^{\mathrm{s}} \eta_{j-})][\sin(\lambda_n^{\mathrm{s}} \eta_{i+}) - \sin(\lambda_n^{\mathrm{s}} \eta_{i-})]}{\lambda_n^{\mathrm{s}2}}. \tag{55}$$

To compute the drawdown in the aquifer during specified H pumping, Eq. (53) is solved for $\overline{q_j}$ and the resulted fluxes are substituted into (48). Note that in this case the drawdown in the aquifer can be computed without explicitly dealing with the wellbore storage term. The flowrate during specified drawdown pumping is computed from the discretized form of (20)

$$\bar{Q} - \alpha\bar{H} = b \sum_{j=1}^{N} \Delta\eta_j \overline{q_j}. \tag{56}$$

Imposing condition (56) on (52) yields the system of equations for a flow-controlled well (specified flowrate pumping)

$$\bar{Q} = \sum_{j=1}^{N} \overline{q_j} [\alpha \Psi_{ij} + b\Delta\eta_j], \tag{57}$$

in matrix form

$$\begin{bmatrix} b\Delta\eta_1+\alpha\Psi_{1,2} & b\Delta\eta_2+\alpha\Psi_{1,2} & \cdots\cdots & b\Delta\eta_N+\alpha\Psi_{1,N} \\ b\Delta\eta_1+\alpha\Psi_{2,1} & b\Delta\eta_2+\alpha\Psi_{2,2} & \cdots\cdots & b\Delta\eta_N+\alpha\Psi_{2,N} \\ \vdots & \vdots & \vdots\ \vdots & \vdots \\ \vdots & \vdots & \vdots\ \vdots & \vdots \\ b\Delta\eta_1+\alpha\Psi_{N,1} & b\Delta\eta_2+\alpha\Psi_{N,2} & \cdots\cdots & b\Delta\eta_N+\alpha\Psi_{N,N} \end{bmatrix} \begin{bmatrix} \bar{q}_1 \\ \bar{q}_2 \\ \vdots \\ \vdots \\ \overline{q_N} \end{bmatrix} = \begin{bmatrix} \bar{Q} \\ \bar{Q} \\ \vdots \\ \vdots \\ \bar{Q} \end{bmatrix}. \tag{58}$$

The drawdown in the aquifer is again computed using (48). The drawdown within the skin is computed by substituting $\bar{q}_j$ into (49).

2.2. Special cases

Solutions for several special cases can be directly obtained from the general solution (48). Alternative solutions for special cases are also derived to numerically verify the general solution under the limiting conditions.

Uniform Radial Flux. For $N=1$, (48) with substitution from (56) reduces to a uniform flux solution that can also be obtained by treating the integrand in (2) as constant.

No-Skin. When the properties of the skin are the same as those of the aquifer, $\xi_n^s = \xi_n^a$ and term G_n (40) equals zero. As a result, (48) and (49) attain the same functional form with K_0 being the only Bessel function retained.

Simplified Skin. A simpler functional form can be obtained if the flow across the skin is approximated by a steady state difference equation (Perina, 2003). This approximation is applicable to a low permeability skin of small thickness only. Vertical flow components and transient flow cannot be ignored within a highly permeable or very thick skin, respectively.

Fully Penetrating Extraction Well. The solution for full penetration can be obtained from (48) by letting $\eta_1=0$ and $\eta_2=1$. An alternative but simpler functional form of the NUF solution, however, is obtainable directly (Appendix A). The radial flux is resolved as a continuous function of depth without discretization. That alternative solution also serves numerically as a comparison test for the NUF solution.

Leaky Aquifer. A confined aquifer with leakage from an overlying unconfined aquifer through an intervening aquitard is here revisited. The drawdown in the unconfined aquifer is negligible, compared to the drawdown in the confined aquifer. The leakage is drawdown-dependent and the solution for the drawdown in the aquifer should be a function of z even for a fully penetrating extraction well (Lee, 1999, p. 134). This definition of leakage as a boundary flux describes more realistically the flow in the aquifer than the conventional treatment of the leakage as a lumped volumetric water production term (Hantush, 1964).

For a leaky aquifer, the top boundary condition changes to a drawdown-dependent boundary-flux condition

$$K_z^a \frac{\partial h}{\partial z} = c_v h \quad \text{at } z=0, \tag{59}$$

where the vertical leakance

$$c_v = \frac{K_c}{b_c} \tag{60}$$

represents the leakage from a confining layer of thickness b_c with vertical hydraulic conductivity K_c. This definition of the leakance term is consistent with definitions reported in the literature (McDonald and Harbaugh, 1988; Lee, 1999). All solutions for the unconfined aquifer can be converted to leaky aquifer solutions by changing a in Eq. (29) to

$$a_c = c_v \frac{b}{K_z^a} \tag{61}$$

The roots of (24) are now time-independent.

Steady State Flow in Leaky Aquifer. Because the upper boundary condition for a leaky aquifer is non-zero, it is possible to obtain a steady-state solution of Eq. (1). Eqs. (36) and (37) become

$$\xi_n^a = \sqrt{\frac{K_z^a}{b^2}\frac{\lambda_n^{a2}}{K_r^a}}, \tag{62}$$

$$\xi_n^s = \sqrt{\frac{K_z^s}{b^2}\frac{\lambda_n^{s2}}{K_r^s}}, \tag{63}$$

and the terms in (20), (56), and (57) associated with α become zero. The steady state drawdown distribution in the aquifer is completely defined by (48) and the relation between the drawdown in the extraction well and the pumping rate is given by (52).

Confined Aquifer. For a confined aquifer, the upper boundary condition changes to zero flux and as $c_v \to 0$ (or $S_y \to 0$), the roots $\lambda_n = n\pi$ are independent of time. This limiting solution can also be derived by the finite Fourier cosine transform (Sneddon, 1995; p. 73) in η (or separation of variables) instead of the GFFC transform.

Drawdown in an Observation Well. The solutions for drawdown at a point in the aquifer presented here are applicable to a piezometer with a short screen. In practice, observation wells with longer screen intervals are used to measure drawdown.

Wellbore storage in an observation well can cause the delay of the drawdown measured inside the observation well casing with respect to the drawdown in the aquifer; the effect of observation well storage on test data is magnified during rapid drawdown change in the aquifer (Moench, 1997; Butler, 1998). The flow of water from the observation well screen into the aquifer can also be restricted by a low permeability skin. While extraction wells are usually developed to reduce the skin effect, frequently much less effort is spent on the development of groundwater monitoring wells that are customarily used as observation wells during aquifer testing. Omitting the delay of the observation well response in aquifer test analysis could affect the estimated value of S_s^a (Black and Kipp, 1977). Tongpenyai and Raghavan (1981) included the wellbore storage and dimensionless skin factors in the extraction and observation wells by considering the angular flow component in their solution for constant flowrate pumping from an extraction well fully penetrating a confined aquifer. Shapiro (1989) considered the flow of groundwater between the observation well and the aquifer in his radial flow solution for an oscillatory response to pumping in highly permeable media. Black and Kipp (1977) and Moench (1997) treated the drawdown delay in an observation well using Hvorslev's (1951) shape factor and recommended conducting a slug test at the observation well to estimate the shape factor directly.

To arrive at an expression that includes the observation well casing and skin radii and the skin conductivity, it is assumed that the flow of water out of the observation well does not affect the flowfield in the aquifer. This assumption implies that the diameter of the observation well casing is small relative to the distance from the pumping well (Shapiro, 1989). Then the drawdown can be treated as constant around the observation well skin-aquifer interface.

An observation well screened between depths z_{ot} and z_{ob}, with screen and casing radii r_{ow} and r_{oc}, respectively, surrounded by a skin of radius r_{os} and horizontal hydraulic conductivity K_{os} is considered here. No storage is assumed within the skin. The skin material is further assumed to have lower hydraulic conductivity than the surrounding aquifer; vertical flow in the skin can then be considered negligible and the flow across the skin can be approximated by a difference equation

$$-\pi r_{oc}^2 \frac{\partial h_{ow}}{\partial t} = \frac{h_{ow} - h_{os}}{\zeta_{ow}}, \tag{64}$$

where

$$\zeta_{ow} = \frac{r_{os} - r_{ow}}{\pi K_{os}(r_{ow} + r_{os})(z_{ob} - z_{ot})}. \tag{65}$$

Eq. (64) is similar in form to the equation used by Moench (1997, Eq. (28)).

The drawdown $\overline{h_{os}}$ is calculated as an average between z_{ot} and z_{ob} along the skin-aquifer interface

$$\overline{h_{os}} = \frac{1}{\eta_{2ow} - \eta_{1ow}} \int_{\eta_{1ow}}^{\eta_{2ow}} \bar{h} \mathrm{d}\eta \quad \text{at } r, \tag{66}$$

where $\bar{h}$ is the appropriate function for point drawdown in the aquifer, to get

$$\bar{h}_{ow} = \frac{1}{(1 + \zeta_{ow}\pi r_{oc}^2 p)(\eta_{2ow} - \eta_{1ow})} \times \int_{\eta_{1ow}}^{\eta_{2ow}} \bar{h} d\eta \quad \text{at } r. \tag{67}$$

The quantity $\zeta_{ow}\pi r_{oc}^2 p$ in (67) constitutes a dimensionless factor related to the delay of the drawdown in the well with respect to the drawdown in the aquifer; as expected, it decreases with time

and increases with increasing r_{oc} and r_{os}, and with decreasing K_{os}. There is no wellbore storage for $r_{oc}=0$ and the observation well is represented by a vertically averaged point drawdown as in traditional solutions (Hantush, 1964). To represent a case with wellbore storage and no skin, setting $r_{os}=r_{ow}$ is not appropriate (the wellbore storage effect would be lost); $K_{os}=K_r^a$ should be used instead.

The observation well skin radius and conductivity become additional unknown parameters in field test analysis. Although explicitly defined in (65), K_{os} and r_{os} cannot be independently resolved from ζ_{ow} estimated through analysis of drawdown data.

2.3. Remarks on specified flowrate and drawdown

The new solutions are applicable to three major types of aquifer tests: constant flowrate, constant drawdown, and slug test. For constant flowrate

$$\bar{Q}=\frac{Q_c}{p}, \tag{68}$$

where Q_c is the constant flowrate from the extraction well; and for constant drawdown

$$\bar{H}=\frac{H_c}{p}, \tag{69}$$

where H_c is the constant drawdown applied at the extraction well. For the instantaneous groundwater removal (or injection) during a slug test

$$\bar{Q}=\pi r_c^2 H_d, \tag{70}$$

where H_d is the initial displacement; this expression should be substituted for $\bar{Q}$ in specified flowrate solutions to obtain a slug test response. Linear superposition in time of (68)–(70) can be used for step-wise representation of variable pumping.

2.4. Aquifer characterisics

The four aquifer parameters K_r^a, K_z^a, S_s^a, and S_y^a and four skin parameters K_r^s, K_z^s, S_s^s, and S_y^s appear in the general well function as a set of eight independent quantities

$$\frac{S_y^a}{K_z^a K_r^s},\quad \frac{S_y^s}{K_z^s K_r^s},\quad \frac{K_z^a}{K_r^a},\quad \frac{K_z^s}{K_r^s},\quad \frac{S_s^a}{K_r^a},\quad \frac{S_s^s}{K_r^s},\quad \frac{S_y^s}{K_z^s},\quad \text{and}\quad \frac{S_y^a}{K_z^a} \tag{71}$$

from which they can be uniquely determined. The saturated thickness b can also be treated as an unknown independent parameter. If b is known, it can be used as an unknown to indirectly ascertain the parameter determinations (Lee et al., 2002).

3. Numerical evaluation

The inverse Laplace transform was evaluated with the Stehfest (1970) method using 10 summation terms. The Stehfest method has been successfully used for inversion of a variety of well functions (Moench and Ogata, 1984; Hyder et al., 1994; Lee, 1999; Lee et al., 2002); however, its accuracy can be erratic at small times or for distant observation wells (Tseng and Lee, 1998).

The roots of Eq. (24) were evaluated to an accuracy of 10^{-10}; the computation of drawdown can quickly deteriorate at a root-finding accuracy of 10^{-7} or worse. The root-finding in (24) can be facilitated by exploring the relation

$$\lambda_n=n\pi+\theta_n,\qquad n=0,1,2,\ldots \tag{72}$$

where $0<\theta_n<\pi/2$. With increasing n, $\theta_n\to 0$ and $\lambda_n\to n\pi$. The n-th root can be bracketed, $0<\theta_n<\theta_{n-1}$, to narrow successively the likely ranges of root λ_n as n increases for a bisectional root-finding method.

Inverse GFFC Transform. The series in (48), (49), and (54) converge oscillatorily to a final value. Because of the oscillation, proper termination of the summations is critical to accurate computation of the functional values. The period of the oscillation is time-dependent; it is, therefore, convenient to express the period in terms of n. The factor $[\sin(\lambda_n\eta_{i+})-\sin(\lambda_n\eta_{i-})]$ in (45) and (55) can be written through trigonometric identity as

$$2\cos\left[\frac{\lambda_n(\eta_{i+}+\eta_{i-})}{2}\right]\sin\left[\frac{\lambda_n\Delta\eta_i}{2}\right]. \tag{73}$$

The cosine and sine terms in the product represent the high and low frequency components, respectively. The low frequency component determines when the summation can be properly terminated. With increasing n and $\lambda_n \to n\pi$, the periodicity of the sine term can be approximated as

$$\frac{n\pi\Delta\eta_i}{2} = m\pi, \tag{74}$$

where m is an even integer. So the period has an 'index' $N_{\sin}$ equal to the integer part of $2/\Delta\eta_i$, i.e.

$$N_{\sin} = \frac{2}{\Delta\eta_i}. \tag{75}$$

Similarly, the 'index' of periodicity for the cosine term is equal to the integer part of $2/(\eta_{i+} + \eta_{i-})$, which is always smaller than $N_{\sin}$. Examination of the series shows that the i, j components of (45) and (55) are harmonics of a fundamental frequency determined by the shortest screen segment $\Delta\eta_i$. Thus the summation needs to be terminated at an n_∞ which is a multiple of $N_{\sin}$ computed from the shortest screen segment. The numerical results to be presented later were obtained using $N_{\sin} \geq 50$.

Screen Segments. To evaluate the effect of segment length or the number of segments, the NUF solution (48) was compared with the solution for a fully penetrating well (85) in Appanedix A. Ten discrete segments of equal length along the well screen were found sufficient to produce identical drawdown in the aquifer at a distance equal to 0.1 b. The 10-segment case (with equal segmental length) required 60 summation terms for a fully penetrating well. Using progressively shorter segments toward the upper and lower ends of a partially penetrating well screen for achieving higher radial flux resolution was found to be expensive in computational time because the necessary terms of the Fourier series increase rapidly.

The matrices in (53) and (58) are diagonally dominant with non-zero diagonal elements; for equal-length segments and for segmental lengths symmetric about mid-screen, the matrices are symmetric. They were inverted by Gaussian elimination.

4. Results and discussion

To generalize the plots refered to in the following discussion, traditional definitions for dimensionless time, drawdown, and flowrate are used when practical. Dimensionles time $1/u$

$$u = \frac{r^2 S_s^a}{4\pi K_r^a t} \tag{76}$$

is used for plotting the drawdown in the aquifer and t_d

$$t_d = \frac{K_r^a t}{r_w^2 S_s^a}, \tag{77}$$

is used for plotting the time-varying flowrate during constant drawdown pumping. Dimensionless drawdown in the aquifer h_d

$$h_d = \frac{2\pi(z_b - z_t)K_r^a h}{\Delta Q} \tag{78}$$

applies to constant flowrate pumping (note that for a fully penetrating well, h_d differs from the quantity used by Theis (1935) by a factor of 2); an alternate definition

$$h_d = \frac{h}{\Delta H} \tag{79}$$

is used for constant drawdown pumping. Dimensionless flowrate during constant drawdown pumping Q_d is

$$Q_d = \frac{Q}{2\pi H K_r^a (z_b - z_t)}. \tag{80}$$

Other factors (K_z/K_r, S_y, well screen) affecting the plotted variables are shown on the figures as applicable. Because of the dependence of drawdown on the length and position of the pumping and observation well screens, and aquifer as well as skin properties, the general well function arguments cannot be combined into a convenient set of dimensionless quantities that uniquely define the functional value.

The following discussion focusses on an unconfined aquifer; the effects of extraction well screen length on flux distribution in a confined aquifer were discussed by Chang and Chen (2003). Drawdown and flowrate for leaky and confined aquifers are shown for comparison.

A comparison of NUF and UF solutions for an unconfined aquifer is made to see if the common assumption of uniform radial flux along the extraction well screen is adequate. The screen interval for the NUF solution was discretized into 10 equal segments

Table 1
Deviations (UF-NUF)/NUF% for different screen placement

Observation depth	Fully penetrating well observation distance			Partially penetrating well pumping well screen intervals			
	0.1*b*	0.25*b*	0.5*b*	0–0.25*b*	0.25*b*–0.5*b*	0.5*b*–0.75*b*	0.75*b*–*b*
0	18.0	12.0	6.7	9.0	2.0	1.0	2.0
0.25*b*	2.5	2.0	1.7	5.5	6.0	6.0	6.0
0.5*b*	−4.0	−4.0	−3.8	−3.5	−3.5	6.0	8.0
0.75*b*	−6.5	−6.0	−5.8	−3.5	−3.5	6.0	8.0
b	−7.2	−7.0	−6.5	−4.0	2.0	6.0	−4.0

The distance of all observations is 0.1*b*. Deviations are time-dependent; only the extrema are listed.

and one screen segment was used for the UF solution. All solutions are evaluated for a well with no skin installed in a hypothetical aquifer 100 m thick, with $K_r^a = 1 \times 10^{-2}$ m/min, $K_z^a/K_r^a = 0.1$, $S_s^a = 1 \times 10^{-4}$, $S_y^a = 0.25$, and $r_w = r_c = 0.15$ m, subject to pumping at a unit constant flowrate or unit constant drawdown. Several scenarios for a fully or partially penetrating well (with a screen 0.25 *b* and 0.5 *b* long) are considered. The results are summarized in Tables 1 and 2 and Figs. 2–5.

Constant Q, Fully Penetrating Extraction Well. The deviation between UF and NUF drawdown at selected depths versus $1/u$ is depicted in Fig. 2a. The maximum deviation occurs during the time of the delayed yield when the vertical flow component in the aquifer is at maximum. At late times, when the horizontal flow in the aquifer dominates, the UF and NUF solutions become identical. The small difference between the two solutions at early times indicates that at the onset of pumping, flow in the aquifer is essentially horizontal.

The UF solution over-predicts drawdown at the screen midpoint and greater depths (i.e. UF > NUF), and under-predicts drawdown at depths closer to the water table (i.e. UF < NUF). The deviation between UF and NUF drawdown is not symmetric about the mid-depth; a deviation of about −18% occurs near the water table while deviation of only 7% occurs near the bottom of the aquifer, reflecting the difference in boundary conditions.

Constant Q, Partially Penetrating Extraction Well. Fig. 2b shows the deviations for pumping from a partially penetrating well with a screen 0.5 *b* long centered across the aquifer. Generally, UF > NUF at depths near the screen midpoint, but UF < NUF toward the two ends of the screen. The deviation between the UF and NUF solutions is, like the cases for a fully penetrating well, at its maximum during the period of delayed yield. Unlike the results for the fully-screened well, the deviations persist to late time.

Constant Q, Other Well Configurations. The deviation of UF from NUF solutions decreases slowly with the radial distance from the extraction well for a given depth of observation (Table 1). For a partially penetrating extraction well, the deviation also depends on the screen location and length. Generally, the deviation is greater nearer the screen depth (Table 1) and decreases with decreasing screen length (not shown).

Fig. 3 depicts the dimensionless drawdown (78) distribution near an extraction well during constant flowrate pumping for the times corresponding to the greatest difference between the UF and NUF solutions. The UF solution over-predicts drawdown near the aquifer bottom and under-predicts drawdown near the water table for pumping from a fully penetrating well (Fig. 3a) and for a well screened across the bottom half of the aquifer thickness (Fig. 3d). For a well screened across the upper half of the aquifer thickness, the UF solution over-predicts drawdown at the screen depth

Table 2
Deviations (UF-NUF)/NUF% for different anisotropy ratios

Observation depth	K_z^s/K_r^s		
	0.01	0.1	1
0	28.0	18.0	13.4
0.25*b*	2.0	2.5	2.0
0.5*b*	−3.7	−4.0	−5.3
0.75*b*	−5.6	−6.5	−7.7
b	−6.2	−7.2	−8.5

Fully penetrating extraction well, $r = 0.1b$. Deviations are time-dependent, only the extrema are listed.

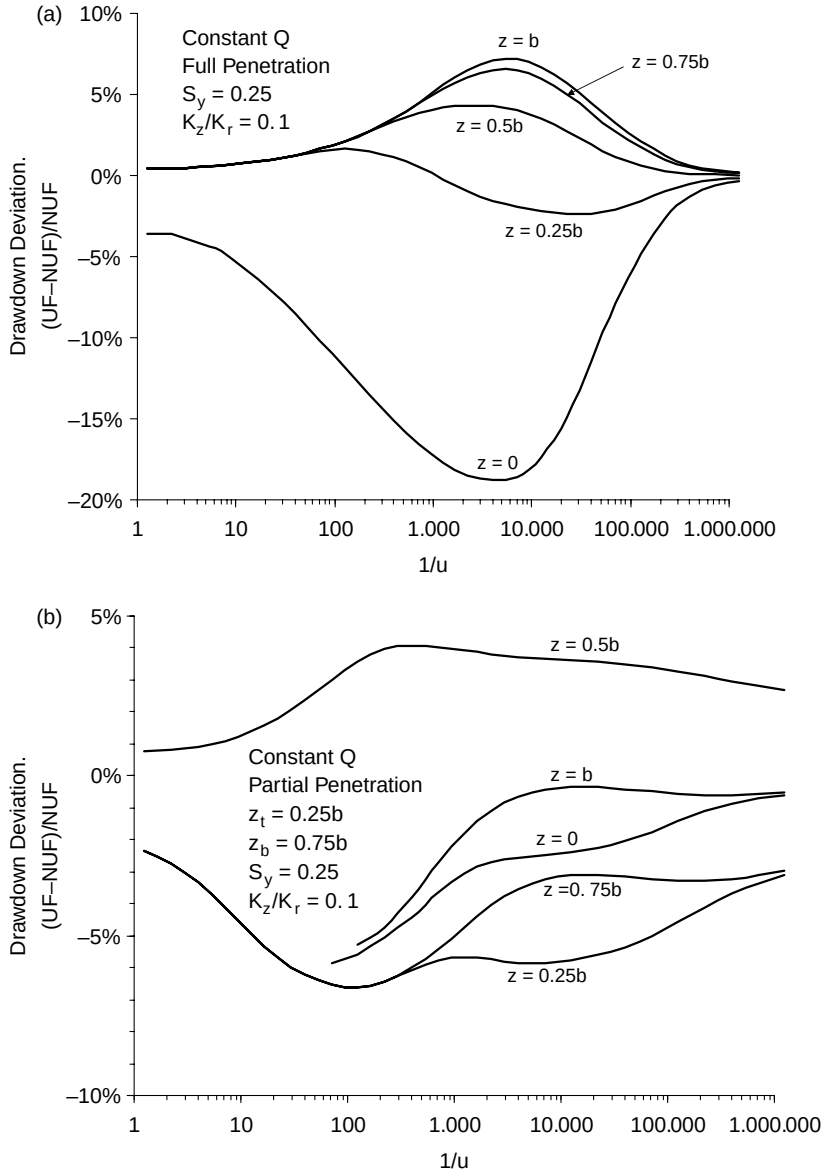

Fig. 2. (a) Deviation of UF from NUF drawdown at different depths during pumping from a fully penetrating well. Note that deviations at all depths converge to zero at late time. (b) Deviation of UF from NUF drawdown at different depths during pumping from a partially penetrating well. Note that all deviations persist to late time.

with the maximum error near the mid-screen depth (Fig. 3b). The difference between the UF and NUF solutions is the smallest for a well screen centered across the aquifer (Fig. 3c).

Constant Q, Effect of K_z^a/K_r^a Ratio. The deviation of UF from NUF solutions decreases with decreasing anisotropy (increasing K_z^a/K_r^a ratio) for observation points near the water table but increases with the observation depth (Table 2).

Constant Q, Radial Flux Distribution. Fig. 4 depicts the distributions of fluxes across the extraction well screen at different times during a constant flowrate pumping. For a fully penetrating well (Fig. 4a), the radial fluxes are initially relatively

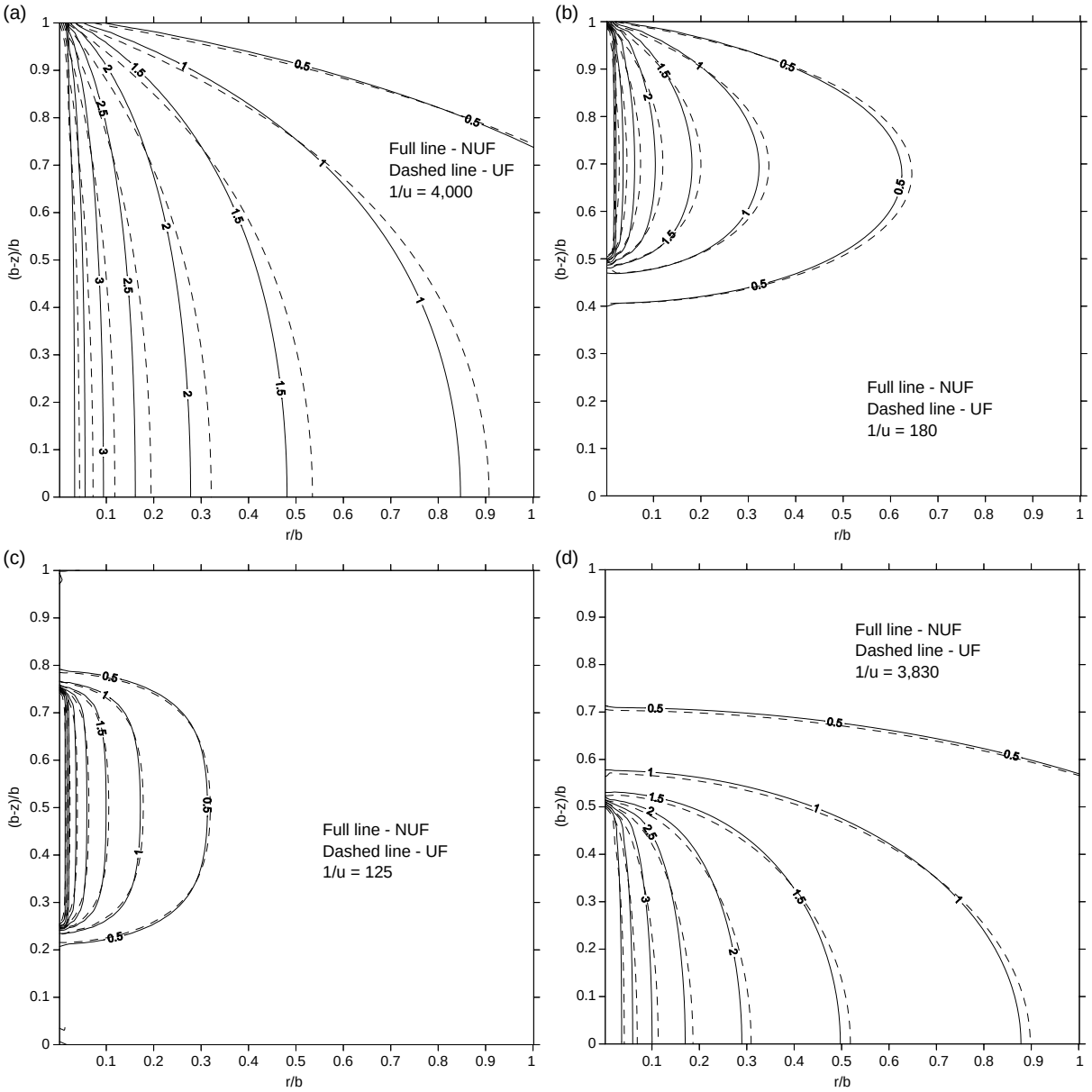

Fig. 3. Comparison of UF and NUF dimensionless drawdown distribution in an unconfined aquifer during constant flowrate pumping for an extraction well screened from (a) -0 to b, (b) -0 to $0.5b$, (c) $-0.25b$ to $0.75b$, (d) $-0.5b$ to b. Note that the difference between UF and NUF drawdown varies with time, illustrated are distributions when the differences are at maxima.

uniform. With increasing vertical flow components due to the drainage at the water table during the period of delayed response (times between 10 and 100 min), the fluxes increase at the top of the screen but decline at the bottom of the screen. At late times (times 10^4 and 10^5 min), as the delayed-yield effect diminishes, the fluxes return to uniformity. The total flow across the screen increases initially with time due to the withdrawal of water from the wellbore but stabilizes soon after 0.1 min. During pumping from a partially penetrating well (Fig. 4b), the radial fluxes are initially uniform along the screen and later increase

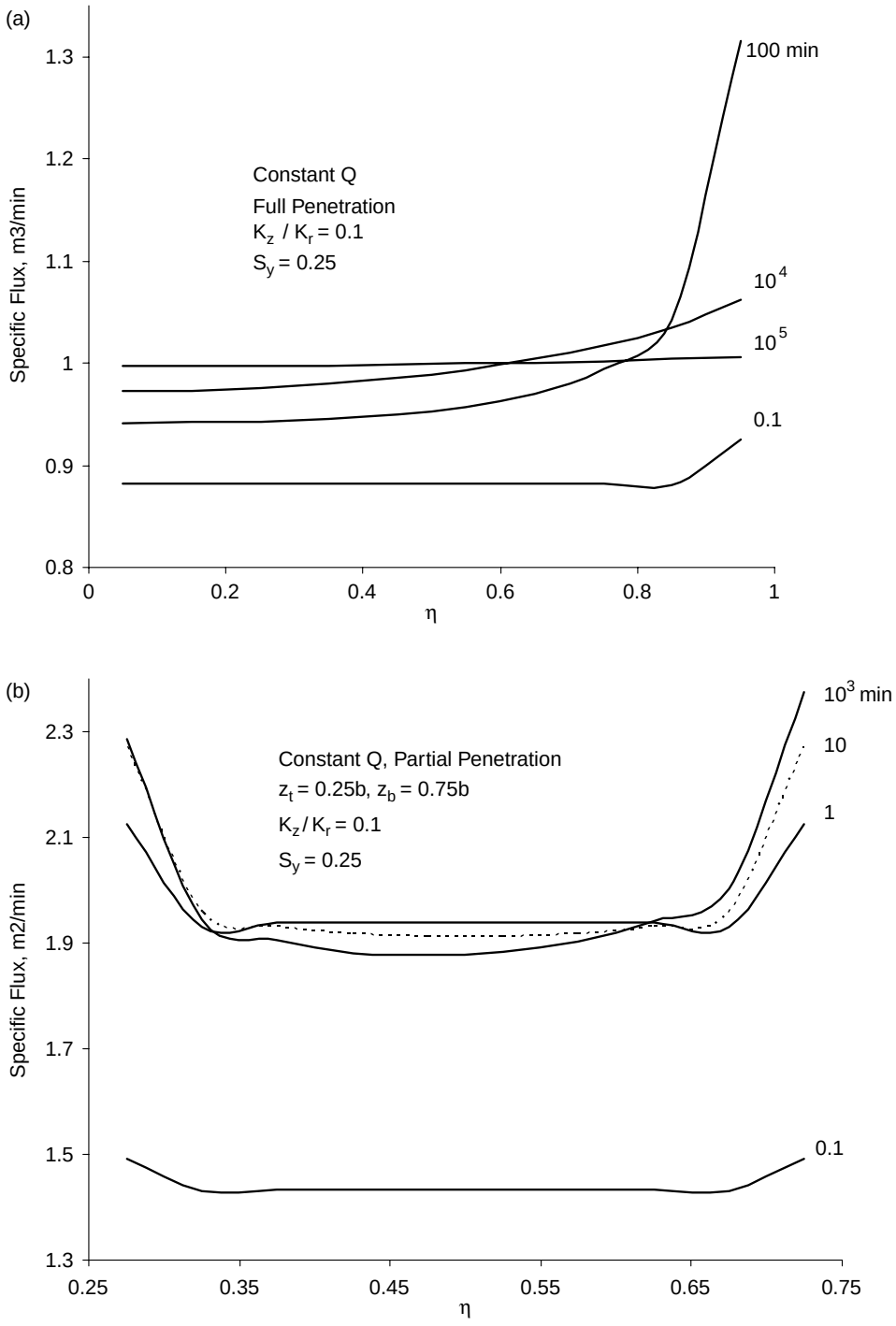

Fig. 4. (a) Variations of radial flux along the screen during constant flowrate pumping from a fully penetrating well. Note the time variation of radial flux as the response transits into and out of the delayed yield period (100–10^4 min). (b) Variations of radial flux along the screen during constant flowrate pumping from a partially penetrating well (screen interval 0.25*b*–0.75*b*).

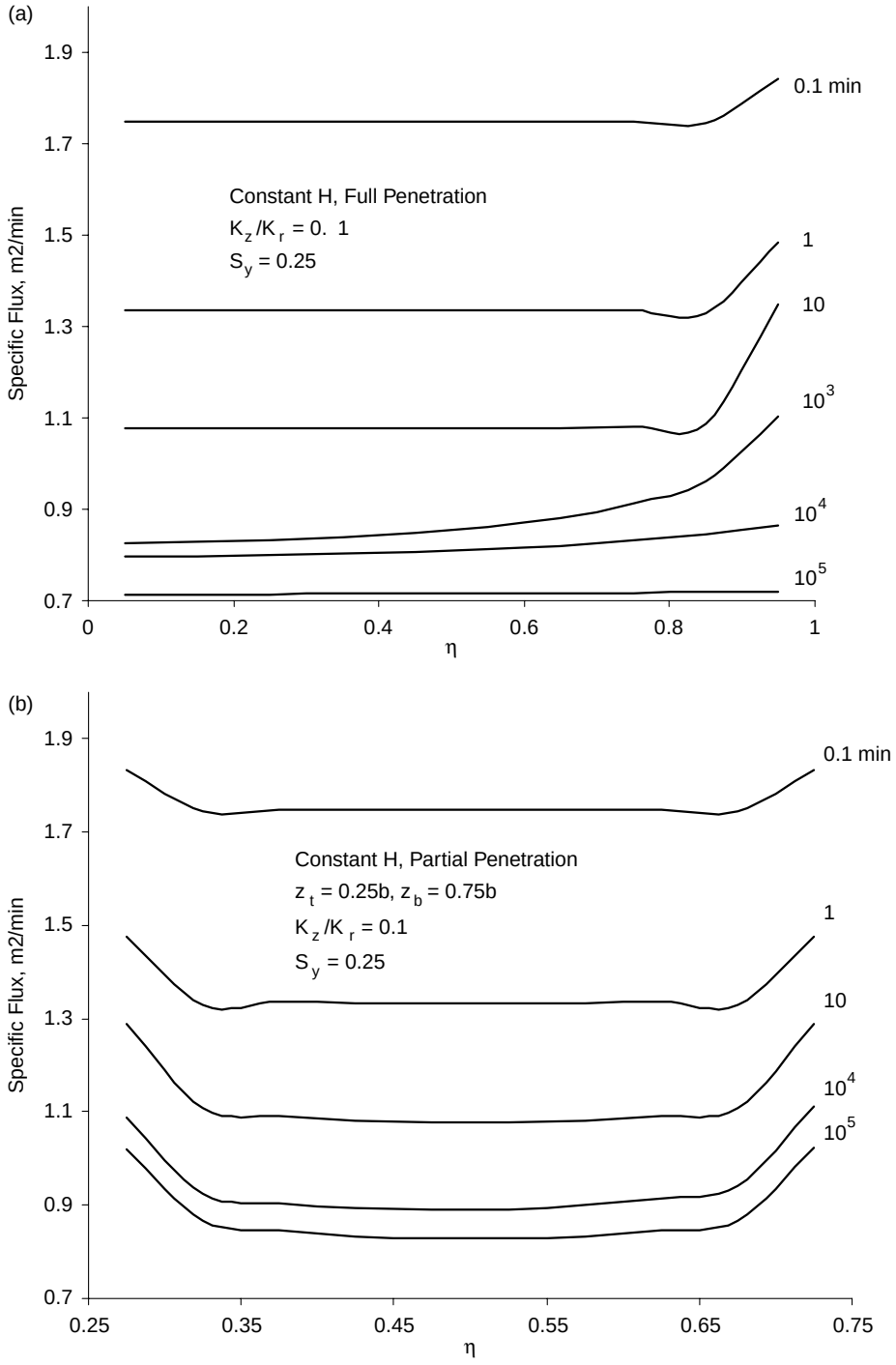

Fig. 5. (a) Variations of radial flux along the screen during constant drawdown pumping from a fully penetrating well. Note the decline of specific flux with time and uniformity at late time. (b) Variations of radial flux along the screen during constant drawdown pumping from a partially penetrating well (screen interval 0.25*b*–0.75*b*). Note the non-uniformity at all times.

near the two screen ends relative to the middle fluxes; this non-uniform flux distribution persists into late times ($>10^3$ min, not shown).

Constant H, Radial Flux Distribution. Fig. 5 shows the distribution of radial fluxes during constant drawdown pumping. In the full-penetration case (Fig. 5a), the fluxes are greater at mid-times (1–10^3 min) at the upper end of the screen relative to the lower end and approach uniformity at late times (10^4 and 10^5 min). In the partial-penetration case (Fig. 5b), the fluxes are uniformly distributed along the central part of the screen but increase toward both ends at all times in contrast to the full-penetration case. In all cases, the radial fluxes decline with time in every segment as a result of declining total flowrate during constant head pumping.

Constant Q, Effect of S_y. Fig. 6 shows the difference between the UF and NUF solutions for drawdown at the water table for different values of specific yield S_y. The differences increase with increasing S_y and are at a maximum during the peak of the delayed yield effect. Similar trends, with smaller discrepancy, also appear for greater observation depths and partially penetrating wells (not shown).

Flowrate and Drawdown in Extraction Well. Besides the drawdown in the aquifer discussed so far, the new solutions allow the examination of the drawdown and flowrate within the extraction well itself. The difference between the UF and NUF solutions is small (not shown) because both solution approaches impose the wellbore storage condition in the integration of (2). Hence, the computationally simpler UF solution is adequate for computing the drawdown in the pumping well during constant flowrate pumping, the flowrate during constant drawdown pumping, and the displacement in the test well during a slug test in most cases.

The time-flowrate curve at constant drawdown pumping (Fig. 7) exhibits a delayed yield effect similar to the phenomena for the constant flowrate pumping from an unconfined aquifer. The flowrate reaches a steady state for pumping from a leaky aquifer; a response for a confined aquifer is also

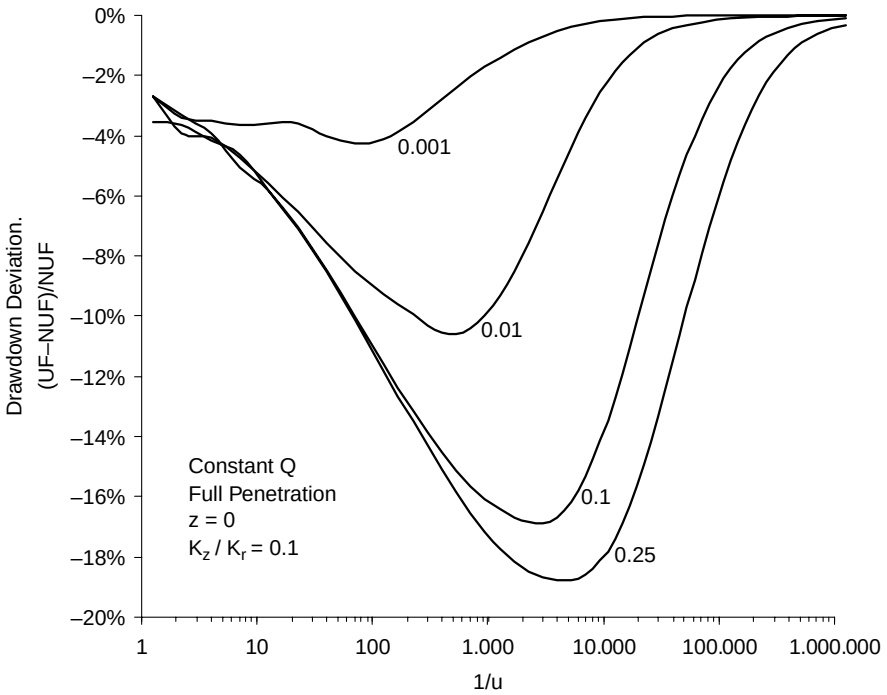

Fig. 6. Deviation of UF from NUF drawdown in the aquifer at the water table during pumping from a fully penetrating well for different values of S_y.

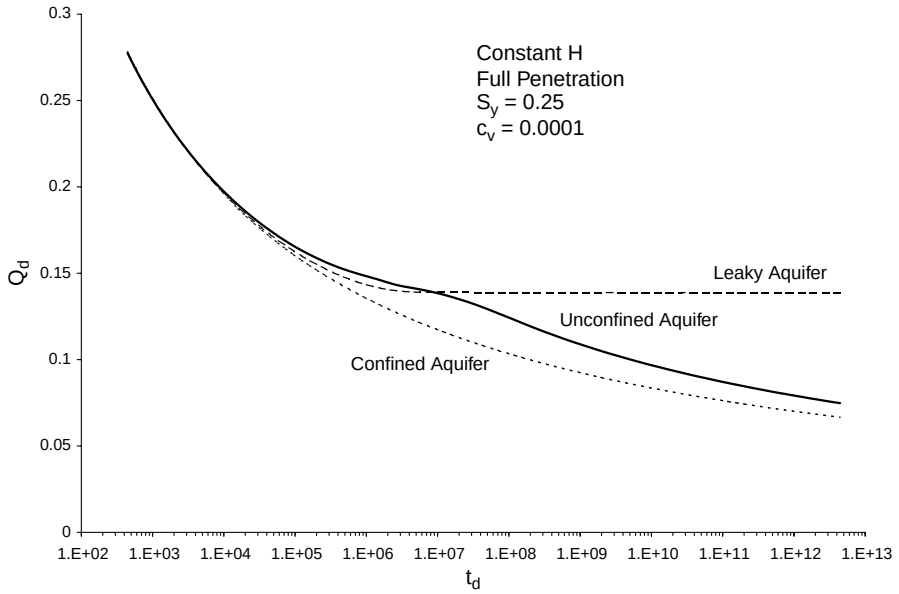

Fig. 7. Time-varying flowrate during constant drawdown pumping from a well fully penetrating a confined, unconfined, and leaky aquifer. The unconfined aquifer response displays a delayed yield effect and becomes sub-parallel to the confined response at late times; the leaky aquifer response becomes steady. Deviation of UF from NUF flowrate is insignificant.

shown for comparison. Note the overlapping of the three curves at early times ($t_d < 10^4$), departure between them at intermediate times (10^4 to 10^7), and leaky aquifer response reaching a steady state, and confined and unconfined responses sub-parallel to each other at late times ($t_d > 10^7$).

Drawdown in an Observation Well. Example plots of the different response of a confined, unconfined, and leaky aquifer to constant flowrate pumping and constant drawdown pumping are shown for fully penetrating wells in Fig. 8. As in the case of the time-flowrate curve (Fig. 7), the three aquifers respond similarly at early times ($1/u < 1$) and then depart. Note that the leaky aquifer response is closer to that of an unconfined aquifer during the early part of the delayed yield period ($1 < 1/u < 1000$). The unconfined aquifer response exhibits a delayed yield effect during constant drawdown pumping as is the case during constant flowrate pumping. The leaky aquifer response reaches a steady state while the curves for the confined and unconfined aquifers become sub-parallel at late times. The time when the leaky aquifer response becomes steady depends on the value of c_v.

The deviation between the UF and NUF drawdown at an observation well of screen length equal to 0.25 b was compared to the deviation at a point in the aquifer located at the observation screen end or midpoint. The deviation for an observation well was generally found to be the same or smaller than the deviation for a point. Drawdown in an observation well with well-bore storage and skin is delayed relative to the drawdown in a well with negligible radius (not shown); Tongpenyai and Raghavan (1981) discussed this effect.

Relation between the Drawdown in the Aquifer during Constant Q and Constant H Pumping. The linear relation in the Laplace domain between the drawdown in the extraction well and the pumping rate (52) translates into a non-linear relation in the time domain. The dimensionless drawdown in the aquifer during constant Q pumping can be reproduced by plotting the ratio of h_d/Q_d during constant H pumping. To obtain proper scaling, the definition of h_d in (78) was modified from the traditional one (Theis, 1935) by a factor of 2 and replacing b by $(z_b - z_t)$.

Multiple Extraction Wells. The drawdown effects of multiple extraction wells operating at specified flowrates can be linearly superimposed. However, the effects of interfering extraction wells pumped in constant-drawdown mode are not linear and their

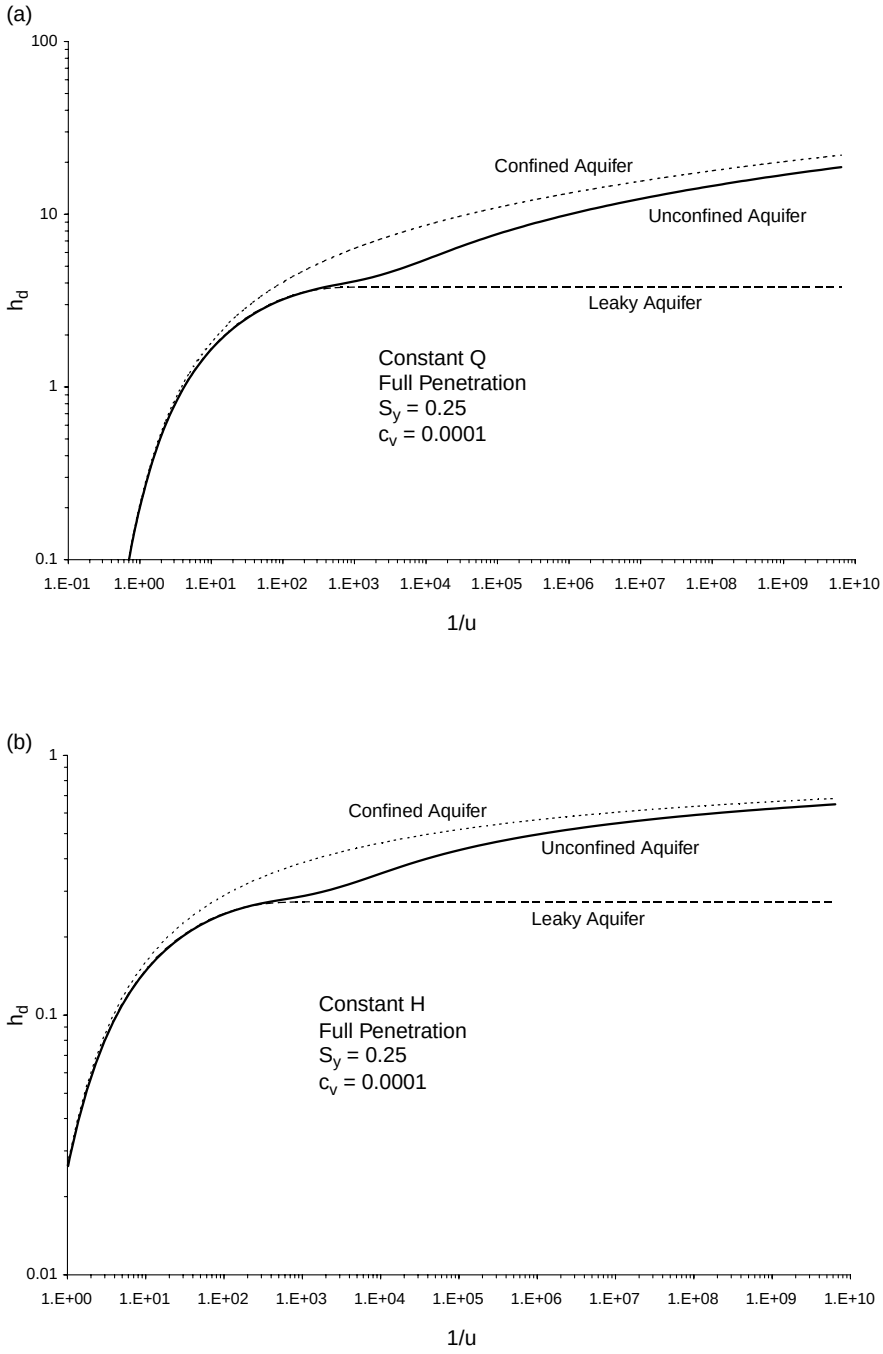

Fig. 8. (a) Drawdown in a fully penetrating observation well during constant flowrate pumping from a fully penetrating well. The confined aquifer response is identical to the Theis function; the unconfined aquifer response displays a delayed yield effect; the leaky aquifer response becomes steady. (b) Drawdown in a fully penetrating observation well during constant drawdown pumping from a fully penetrating well. Note the drawdown in a confined and unconfined aquifer approaching H while the leaky aquifer response becomes steady. The unconfined aquifer response displays a delayed yield effect.

extraction rates and drawdown in the aquifer cannot be estimated by superimposing the effects of individual wells (Karadi, 1972) as in the case of constant rate pumping.

5. Conclusions

The solution (48) with relation (56) constitutes a general well function for non-uniform radial flux toward a pumping well that partially penetrates an unconfined aquifer of Neuman type or leaky aquifer of Lee (1999) under the condition of specified well discharge rate or specified drawdown in the extraction well. In the Laplace domain, the two subsets of solutions are interchangeable, irrespective of time dependency. The pumping well may have a skin of finite thickness. The general function (48) reduces to a number of special-case solutions for constant flowrate pumping, constant drawdown pumping, slug test, well with no skin, uniform radial flux along the extraction well screen, and the solution is also applicable to a confined aquifer. The solution accounts for the wellbore storage and skin in an observation well. A different but simpler functional form in (85) and (88) for a fully penetrating extraction well was also derived as a check for the more complicated solution.

Numerical experiments indicate the deviations of UF from NUF drawdown increases with the extraction screen length and increasing S_y^a. The deviation is largest during the time of the delayed yield. At late times, the difference persists for a partially penetrating well while for a fully penetrating well, the NUF and UF solutions converge as the flow in the aquifer becomes essentially horizontal. The difference also depends on the placement of the pumping well screen, the observation location in the aquifer, and K_z^a/K_r^a. For partially penetrating extraction wells, the deviation is at minimum for observation wells screened at the same depth interval as the pumping well.

Acknowledgements

The authors wish to thank two anonymous reviewers whose comments helped improve the manuscript.

Appendix A. Fully penetrating well

For a fully penetrating well, the mixed boundary condition at the well face is replaced by a prescribed drawdown condition. The flux along the extraction well screen is non-uniform and can be evaluated directly without discretization.

The problem is defined by Eq. (13), boundary conditions (14)–(16), (18) and (19), and prescribed drawdown condition at the screen-skin interface

$$\bar{h}^s(r_w,\eta,p)=\bar{H}. \tag{81}$$

Taking the GFFC transform of Eq. (13) and boundary conditions (14) and (15), and applying condition (16) results in (34) and (35) with coefficients A_n and C_n defined by (39) and (38), respectively. Coefficient B_n is evaluated from the GFFC transform of boundary condition (81)

$$B_n=\bar{H}\frac{\sin(\lambda_n^s)}{\lambda_n^s}[K_0(\xi_n^s r_w)+G_n I_0(\xi_n^s r_w)]^{-1} \tag{82}$$

Then

$$\bar{h}_n^a=\bar{H}\frac{\sin(\lambda_n^s)}{\lambda_n^s}\times\frac{K_0(\xi_n^s r_s)+G_n I_0(\xi_n^s r_s)}{[K_0(\xi_n^s r_w)+G_n I_0(\xi_n^s r_w)]K_0(\xi_n^a r_s)}K_0(\xi_n^a r) \tag{83}$$

and

$$\overline{h_n^s}=\bar{H}\frac{\sin(\lambda_n^s)}{\lambda_n^s}\frac{K_0(\xi_n^s r)+G_n I_0(\xi_n^s r)}{K_0(\xi_n^s r_w)+G_n I_0(\xi_n^s r_w)}. \tag{84}$$

Applying the inverse GFFC transform provides the drawdown in the aquifer

$$\bar{h}^a=\bar{H}2a^a\sum_{n=0}^{\infty}\frac{\cos(\lambda_n^a\eta)}{a^a+\sin^2(\lambda_n^a)}\frac{\sin(\lambda_n^s)}{\lambda_n^s}\times\frac{K_0(\xi_n^s r_s)+G_n I_0(\xi_n^s r_s)}{[K_0(\xi_n^s r_w)+G_n I_0(\xi_n^s r_w)]K_0(\xi_n^a r_s)}K_0(\xi_n^a r) \tag{85}$$

and in the skin

$$\overline{h^{\mathrm{s}}} = \bar{H} 2a^{\mathrm{s}} \sum_{n=0}^{\infty} \frac{\cos(\lambda_n^{\mathrm{s}}\eta)}{a^{\mathrm{s}} + \sin^2(\lambda_n^{\mathrm{s}})} \frac{\sin(\lambda_n^{\mathrm{s}})}{\lambda_n^{\mathrm{s}}} \times \frac{K_0(\xi_n^{\mathrm{s}} r) + G_n I_0(\xi_n^{\mathrm{s}} r)}{K_0(\xi_n^{\mathrm{s}} r_{\mathrm{w}}) + G_n I_0(\xi_n^{\mathrm{s}} r_{\mathrm{w}})}. \quad (86)$$

The flow across the well screen is evaluated from the equivalent of (2) for a fully-penetrating well

$$\bar{Q} - \alpha\bar{H} = -2\pi r_{\mathrm{w}} K_{\mathrm{r}}^{\mathrm{s}} \int_0^b \frac{\partial \overline{h^{\mathrm{s}}}}{\partial r} \mathrm{d}z \quad \text{at } r = r_{\mathrm{w}}, \quad (87)$$

to obtain the relation between Q and H

$$\bar{H} = \frac{\bar{Q}}{\alpha + \Pi}, \quad (88)$$

where

$$\Pi = 4a^{\mathrm{s}} b\pi r_{\mathrm{w}} K_{\mathrm{r}}^{\mathrm{s}} \sum_{n=0}^{\infty} \frac{\sin^2(\lambda_n^{\mathrm{s}})}{\lambda_n^{\mathrm{s}2}} \frac{\xi_n^{\mathrm{s}}}{a^{\mathrm{s}} + \sin^2(\lambda_n^{\mathrm{s}})} \times \frac{K_1(\xi_n^{\mathrm{s}} r_{\mathrm{w}}) - G_n I_1(\xi_n^{\mathrm{s}} r_{\mathrm{w}})}{K_0(\xi_n^{\mathrm{s}} r_{\mathrm{w}}) + G_n I_0(\xi_n^{\mathrm{s}} r_{\mathrm{w}})}. \quad (89)$$

Substitution of (88) into (85) or (86) is then used to obtain an equation for drawdown in the aquifer or skin, respectively, during specified flowrate pumping.

The flux q in the radial direction across the well screen during specified drawdown pumping is

$$\bar{q} = 4\pi a^{\mathrm{s}} r_{\mathrm{w}} K_{\mathrm{r}}^{\mathrm{s}} \bar{H} \sum_{n=0}^{\infty} \frac{\cos(\lambda_n^{\mathrm{s}}\eta)}{a^{\mathrm{s}} + \sin^2(\lambda_n^{\mathrm{s}})} \times \frac{\sin(\lambda_n^{\mathrm{s}})}{\lambda_n^{\mathrm{s}}} \xi_n^{\mathrm{s}} \frac{K_1(\xi_n^{\mathrm{s}} r_{\mathrm{w}}) - G_n I_1(\xi_n^{\mathrm{s}} r_{\mathrm{w}})}{K_0(\xi_n^{\mathrm{s}} r_{\mathrm{w}}) + G_n I_0(\xi_n^{\mathrm{s}} r_{\mathrm{w}})}. \quad (90)$$

Substitution for $\bar{H}$ from (88) into (90) yields the radial flux during specified flowrate pumping. Unlike the result for a partially penetrating well, the radial flux is a continuous function of z.

References

Black, J.H., Kipp Jr.., K.L., 1977. Observation well response time and its effect upon aquifer test results. J. Hydrol. 34, 297–306.

Butler Jr., J.J., 1998. The Design, Performance, and Analysis of Slug Tests. CRC Press, Boca Raton, FL. 252 p.

Cassiani, G., Kabala, Z.J., 1998. Hydraulics of a partially penetrating well: solution to a mixed-type boundary value problem via dual integral equations. J. Hydrol. 211, 100–111.

Chang, C.C., Chen, C.S., 2003. A flowing partially penetrating well in a finite-thickness aquifer: a mixed-type initial boundary value problem. J. Hydrol. 271, 101–118.

Churchill, R.V., 1972. Operational Mathematics, 3rd edition McGraw-Hill Book Company, New York pp. 481.

Hantush, M.S., 1961. Drawdown around a partially penetrating well. J. Hydrol. Div., Proc. Am. Soc. Civil Eng. 87 (4), 83–98.

Hantush, M.S., 1964. Hydraulics of wells. In: Hantush, M.S., Chow, V.T. (Eds.), Advances in Hydroscience, vol. 1. Academic Press, New York, pp. 281–432.

Hemker, C.J., 1999. Transient well flow in vertically heterogeneous aquifers. J. Hydrol. 225, 1–18.

Hvorslev M.J., 1951. Time lag and soil permeability in ground-water observations. Bull. No. 36, Waterways Exper. Sta. Corps of Engrs, U.S. Army, Vicksburg, Mississippi, 1–50.

Hyder, Z., Butler Jr.., J.J., McElvee, C.D., Liu, W., 1994. Slug tests in partially penetrating wells. Water Resour. Res. 30 (11), 2945–2957.

Karadi, G., 1972. Technical note: performance of well-groups at constant drawdown. Water Resour. Bull. 8 (6), 1277–1279.

Kawecki, M.W., 1995. Meaningful interpretation of step-drawdown tests. Ground Water 33 (1), 23–32.

Lee, T.C., 1999. Applied Mathematics in Hydrogeology. Lewis Publishers, New York. 382 p.

Lee, T.C., Damiata, B.N., 1995. Distortion in resistivity logging at shallow depth. Geophysics 60 (4), 1058–1069.

Lee, T.C., Perina, T., Lee, C.Y., 2002. Validation of parameter determination by extrapolation and spiking aquifer thickness as an unknown. J. Hydrol. 265, 15–33.

McDonald, G., Harbaugh, A.W., 1988. A Modular Three-Dimensional Finite-Difference Ground-Water Flow Model. Tech. Water Resour. Invest. U.S. Geological Survey, Book 6, A1.

Mishra, S., Guyonnet, D., 1992. Analysis of observation-well response during constant-head testing. Ground Water 30 (4), 523–528.

Moench, A.F., 1997. Flow to a well of finite diameter in a homogeneous, anisotropic water table aquifer. Water Resour. Res. 33 (6), 1397–1407.

Moench, A.F., 1998. Correction to Flow to a well of finite diameter in a homogeneous, anisotropic water table aquifer by Allen Moench. Water Resour. Res. 34 (9), 2431–2432.

Moench, A.F., Ogata, A., 1984. Analysis of constant discharge wells by numerical inversion of Laplace transform solutions. In: Rosenshein, J., Bennett, G.D. (Eds.), Groundwater Hydraulics Water Resource Monograph, vol. 9. AGU, Washington, DC, pp. 146–170.

Neuman, S.P., 1972. Theory of flow in unconfined aquifers considering delayed response of the watertable. Water Resour. Res. 8, 1031–1045.

Neuman, S.P., 1973. Supplementary comments on Theory of flow in unconfined aquifers considering delayed response of the watertable. Water Resour. Res. 9, 1102–1103.

Neuman, S.P., 1974. Effect of partial penetration on flow in unconfined aquifers considering delayed gravity response. Water Resour. Res. 10 (2), 303–312.

Perina T., 2003. Analytical solutions for groundwater and soil vapor flow to a partially penetrating well with non-uniform radial flux along the screen. Doctoral Dissertation. University of California Riverside; 2003.

Press, W.H., Teukolski, S.A., Vetterling, W.T., Flannery, B.P., 1992. Numerical Recipes in FORTRAN: The Art of Scientific Computing. Cambridge University Press, New York pp. 963.

Rasmussen, T.C., Crawford, L.A., 1997. Identifying and removing barometric pressure effects in confined and unconfined aquifers. Ground Water 35 (3), 502–511.

Shapiro, A.M., 1989. Interpretation of ocsillatory water levels in observation wells during aquifer tests in fractured rock. Water Resour. Res. 25 (10), 2129–2137.

Sneddon, I.N., 1995. Fourier Transforms. Dover Publications, New York pp. 542.

Stehfest, H., 1970. Numerical inversion of Laplace transforms. Commun. ACM 13 (1), 47–49.

Theis, C.V., 1935. The relation between the lowering of the piezometric surface and the rate and duration of discharge of a well using groundwater storage. Am. Geophys. Union Trans. 16, 519–524.

Tongpenyai, Y., Raghavan, R., 1981. The effect of wellbore storage and skin on interference test data. J. Petrol. Technol. 33 (1), 151–160.

Tseng, P.H., Lee, T.C., 1998. Numerical evaluation of exponential integral: Theis well function approximation. J. Hydrol. 205, 38–51.